2219-T87铝合金搅拌摩擦焊接头组织与力学性能

王春炎[1], 曲文卿[1], 姚君山[2], 赵海云[1]
(1. 北京航空航天大学 机械工程与自动化学院, 北京 100191;
2. 上海航天设备制造总厂, 上海 200245)

王春炎

摘 要: 采用搅拌摩擦焊方法对 8 mm厚 2219-T87铝合金进行了焊接. 对接头的宏观形貌、微观组织、显微硬度及断口形貌进行了分析. 结果表明, 焊核区为细小的等轴晶粒, 晶粒尺寸远小于母材; 热机影响区发生了弯曲变形; 热影响区组织出现了明显粗化. 前进边热机影响区和焊核区形成明显分界线, 后退边相对模糊. 搅拌摩擦焊对接头各区域沉淀相分布形态有重要影响. 接头室温拉伸强度可以达到母材的 70% 以上. 沿焊缝横截面的显微硬度的分布显示, 硬度最低点位于后退侧热影响区区域, 断裂位置位于后退侧热影响区处, 接头的断裂形式为韧性断裂.

关键词: 2219铝合金; 搅拌摩擦焊(FSW); 力学性能; 微观组织
中图分类号: TG115.5 文献标识码: A 文章编号: 0253-360X(2010)10-0077-04

0 序 言

2219铝合金在 −250 ~250 ℃的温度范围内, 具有良好的比强度、抗应力腐蚀性以及良好的力学性能, 在航天工业中受到青睐[1], 根据目前的情况, 用 2219铝合金取代 2A14铝合金作为航天贮箱材料尤为必要[2]. 对 2219铝合金的焊接国外曾采用熔化极气体保护焊(MIG)、钨极氩弧焊(TIG)、电子束焊(EBW)、变极性等离子弧焊(VPPAW)等多种熔焊方法.

搅拌摩擦焊接技术是英国焊接研究所 1991发明的一种新型固相连接技术[3]. FSW解决了传统熔焊易出现的问题, 且接头性能高, 在铝合金焊接方面发展迅速[4−6], 目前已被确认为新一代运载火箭贮箱的关键制造工艺. 全面了解 2219铝合金搅拌摩擦焊技术对于贮箱方案设计以及新一代贮箱材料的理论研究有着重要意义.

重点对 2219-T87铝合金搅拌摩擦焊接头进行了室温力学性能的试验研究, 获得了 2219-T87铝合金及其搅拌摩擦焊接头的室温力学性能, 并且对 2219铝合金母材及 FSW接头微观组织和拉伸断口形貌进行了分析. 讨论了 FSW对 2219-T87铝合金拉伸力学性能的影响, 为 2219铝合金 FSW焊提供了相应的参考与支持.

收稿日期: 2009-06-15

1 试验方法

试验材料为 2219(Al-Cu-Mn系)高强铝合金板材, 热处理状态为 T87, 即固溶处理+7%冷变形+人工时效. 材料厚度为 8 mm, 其化学成分列于表 1, 主要强化元素有: Cu, Mn, 2219铝合金属 Al-Cu-Mn系可热强化铝合金. 试验选用螺旋形搅拌头, 搅拌针直径为 8 mm, 轴肩直径为 24 mm, 搅拌针长度为 7 mm. 焊接时旋转速度为 500 ~800 r/min, 焊接速度为 100 ~200 mm/min.

表 1 2219-T87铝合金的化学成分(质量分数, %)
Table 1 Chemical composition of aluminum alloy 2219-T87

Cu	Mn	Fe	Ti	V	Zn	Si	Zr	Al
6.48	0.32	0.23	0.06	0.08	0.04	0.49	0.20	余量

焊后沿试样横截面(轧制方向)截取试样, 用混合酸(1.0% HF+1.5% HCL+2.5% HNO_3 +95.0% H_2O)对抛光后的试样进行腐蚀, 在光学显微镜下观察母材和 FSW焊接接头的微观组织. 用 HXZ-1000数字式显微硬度计测量焊接接头的显微硬度; 按国家标准 GB/T 2649—1989《焊接接头机械性能试验取样方法》和 GB/T 228—2002《金属材料室温拉伸试验方法》沿板材轧制方向制取拉伸试样, 分别在 MTS-880力学性能试验机上进行室温拉伸试验, 拉伸速率为 2 mm/min, 每组拉伸试验结果取 8

个试样的平均值. 用 JSM-5800扫描电镜观察母材及焊接接头的拉伸断口形貌.

2 试验结果与分析

2.1 搅拌摩擦焊接头的微观组织

图 1为 2219-T87铝合金搅拌摩擦焊的横截面宏观形貌, 将接头分为以下 4个区域: A为焊核区 (nugget zone, 简称 NZ), B为热机影响区 (thermo-mechanically affected zone, 简称 TMAZ), C为热影响区 (heat-affected zone, 简称 HAZ), D为母材 (base metal, 简称 BM).

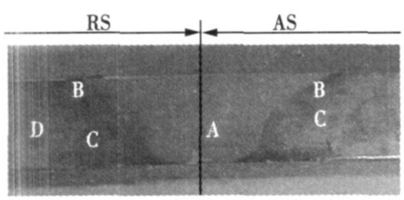

图 1 2219-T87铝合金 FSW接头横截面宏观形貌
Fig. 1 Cross-section morphology of friction stir weld (FSW) of aluminum alloy 2219-T87

FSW时旋转的搅拌头在焊缝方向的切线速度与焊接速度方向相同的一侧称为前进侧 AS (advancing side), 而相反的一侧称为后退侧 RS (retreating side). 由图 1可知, 焊核和热机影响区的分界线在前进侧和后退侧不同, 前进侧分界明显, 后退侧相对模糊. 出现这种现象可能与焊接过程中两侧金属的塑性流动状态的差别有关[7-9].

图 2为 2219-T87铝合金搅拌摩擦焊接头各区域显微组织, 图 2a~图 2d分别为母材区、焊核区、热机影响区及热影响区.

母材的主要相组成物为 α 固溶体、θ ($CuAl_2$)相和 T相 ($CuMn_2Al_{12}$), 并有少量的 $TiAl_3$. 由图 2a可以看到母材为板条组织, 有明显的轧制痕迹, 在母材的晶界和晶内存在大量的强化相. 焊前母材晶粒细长, 平均长度为 75 μm, 宽度为 18 μm. 焊核区受到焊接热循环及搅拌双重作用, 形态发生明显变化. 在搅拌摩擦焊接过程中, 搅拌针与工件及搅拌头肩部与工件之间产生大量的热量, 使周围金属塑化并充分流动, 位错在搅拌力作用下密度不断增加, 当储存能增加到一定程度, 足够发生再结晶时, 金属内便开始不断形成晶核, 组织发生动态再结晶, 由原母材的板条状组织转变为等轴再结晶组织, 晶粒均匀细小, 平均尺寸为 6 μm (图 2b). 热机影响区受到搅拌针以及轴肩的共同作用, 且经受了较高温度的焊

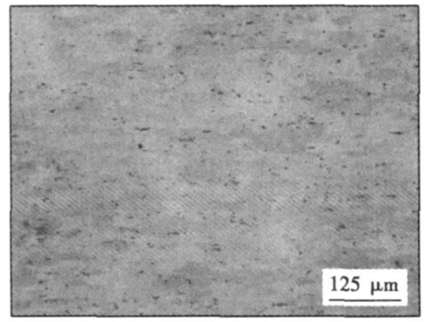

(a) 母材

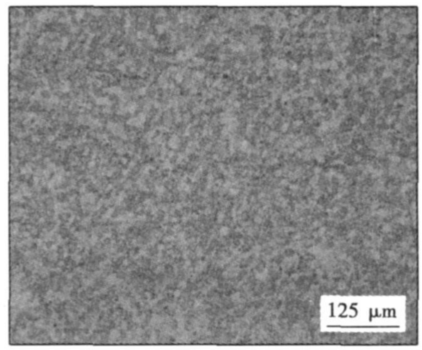

(b) 焊核

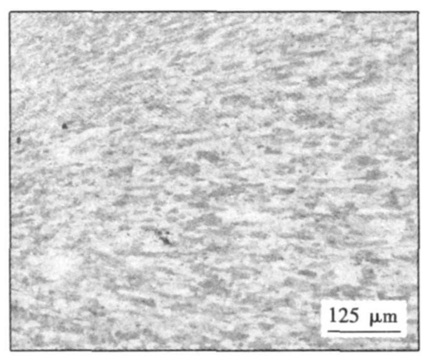

(c) 热机影响区

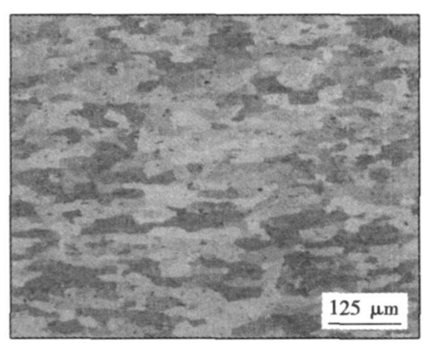

(d) 热影响区

图 2 2219-T87铝合金 FSW接头各区域微观组织
Fig. 2 Microstructures of FSW joint of 2219-T87

接热循环, 晶粒发生了较大的弯曲变形, 由图 2c所示, 组织有明显被拉长迹象, 平均长度为 110 μm, 宽度为 6 μm. 热影响区微观组织如图 2d所示, 由于在焊接过程中没有受到搅拌作用, 但是在焊接过程中受到热循环的作用, 晶粒明显粗大, 但仍保留了板

条状组织的特征.

接头析出相受到焊接热循环和搅拌作用的影响，在接头各区域的分布形态存在明显差异. 图 3为 2219-T87铝合金搅拌摩擦焊接扫描电镜图. 2219铝合金是以 α(Al)为基体，含有许多小颗粒，对白色颗粒进行了电子能谱分析(EDS分析)，结果见表 2，白色颗粒为 $CuAl_2$相. 由图 3a可以看出，母材晶界和晶界内弥散分布着细小的尺寸在 10 μm以下的析出相. 与母材相比，焊核区沉淀相更加细小，尺寸在 4 μm以下，沉淀相尺寸大小不一，其中颗粒尺寸较大的、形状不规则的是原基体粗大 θ相破碎的结果，细小的颗粒主要是变形再结晶的析出相 (图 3b). 热机影响区温度没有焊核区高，但作用时间较长，经搅拌作用及焊接热循环，晶粒被明显拉长，发生局部动态再结晶，部分沉淀相粒子发生再次固溶、析出和长大 (图 3c). 可见搅拌头的搅拌作用降低了焊核区和热机影响区沉淀相的尺寸. 热影响区没有受到机械搅拌作用，故聚集的颗粒最大，析出相明显粗化，达到 16 μm左右，未发现析出相溶解的现象 (图 3d).

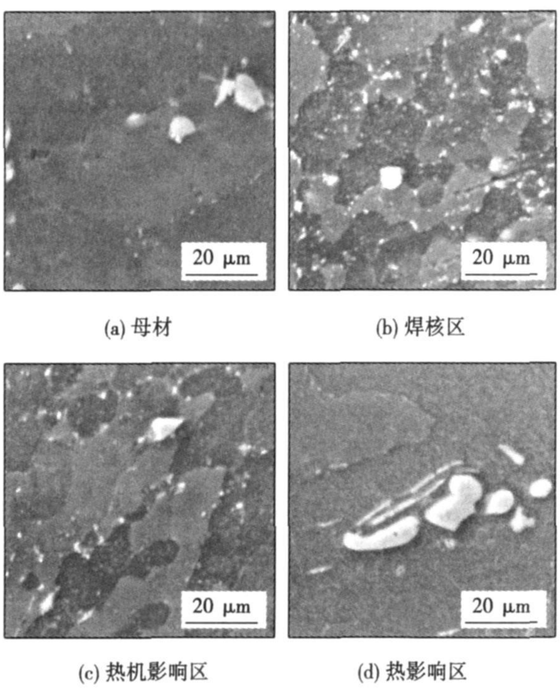

(a) 母材　(b) 焊核区
(c) 热机影响区　(d) 热影响区

图 3　2219-T87铝合金 FSW接头各区域扫描电镜图
Fig. 3　SEM of FSW joint for 2219-T87

表 2　沉淀相的能谱分析(EDS)
Table 2　EDS of precipitates

元素	原子分数(%)
Al	62.80
Cu	37.20

2.2　搅拌摩擦焊接头的拉伸力学性能

拉伸性能测试结果见表 3. 由表可见，无论何种焊接方法均使母材强度以及塑性有很大的降低. 但 FSW焊接接头的性能明显优于 VPTIG焊接接头. FSW室温下的接头系数达到 70%以上，而 VPTIG的接头系数不到 60%. 可见 FSW作为一种新兴的固相连接方法，无论是从强度还是塑性来看，力学性能明显优于传统的熔焊方法.

表 3　2219-T87铝合金母材及焊接接头拉伸测试结果
Table 3　Mechanical properties of base metal and FSW joint

状态	抗拉强度 R_m/MPa	屈服强度 R_{eL}/MPa	断后伸长率 A(%)
母材	458.4	387.5	12.8
FSW	321.3	153.2	6.3
VPTIG	255.8	133.3	2.9

从断后宏观形貌来看，FSW断裂位置多位于后退侧热影响区处，图 4为 2219-T87铝合金 FSW断裂位置图.

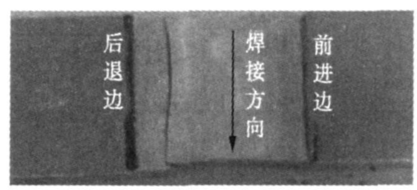

图 4　FSW拉伸断口
Fig. 4　Macrofractography of FSW joint

2.3　搅拌摩擦焊接接头的硬度分布

焊缝横截面的硬度分布如图 5所示. FSW接头各区域硬度分布是不均匀的，即母材硬度最高，热机影响区和热影响区硬度降低，到焊核处硬度又升高，但低于母材的硬度，最低点位于后退侧热影响区，拉

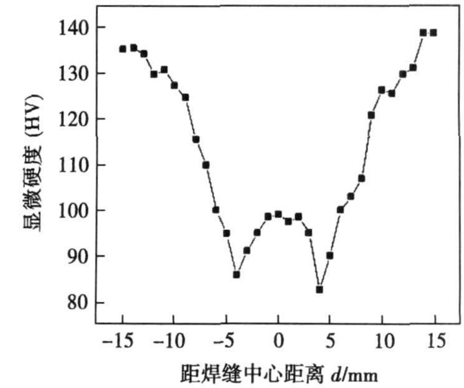

图 5　接头硬度分布
Fig. 5　Micro-hardness of FSW joint

伸试验结果也较好的证明了这点, 断裂位置多位于后退侧热影响区.

结合图 2的微观组织变化, 可看出焊接接头各区域硬度的变化与组织的变化是紧密联系的. 热影响区可能是由于受到高温的作用, 稳定相 θ 质点聚集长大, 材料出现了过时效, 使强度下降, 硬度降低[10]. 焊核区由于晶粒特别细小, 所以强度有所提高.

2.4 断口分析

图 6a, b分别为母材和 FSW接头高倍断口微观形貌图. 可以看出母材由大小不一的韧窝和撕裂岭组成, 韧窝较大, 较深, 撕裂岭较多, 断口为塑性断口. FSW拉伸断口为大面积的等轴韧窝和撕裂棱组成, 为韧性断裂. 与母材断口相比, 韧窝较小、较浅, 分布比较均匀, 且韧窝的底部发现沉淀相. 韧窝的大小与第二相粒子或杂质有关, 由于受到搅拌头的机械搅拌作用, 使沉淀相破碎, 形成细小颗粒状的沉淀相, 这些细小沉淀相剥离后留下非常细小的光滑韧窝. 图 6b黑色粒子为沉淀相颗粒.

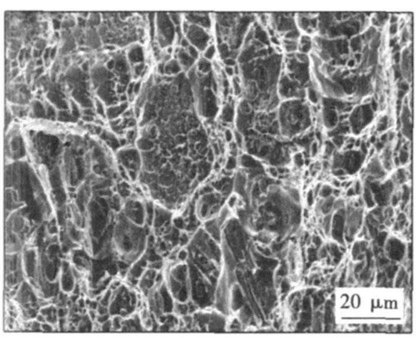

(a) 母材断口

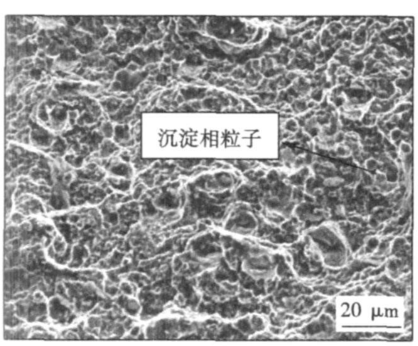

(b) FSW断口

图 6 拉伸断口形貌
Fig. 6 Magnified fractographs

3 结 论

(1) 经微观组织分析, 搅拌摩擦焊接头的微观组织分四个区域, 即焊核区、热机影响区、热影响区和母材区. 焊核和热机影响区的分界线在前进侧和后退侧不同, 前进侧分界明显, 后退侧相对模糊. 接头各区域微观组织存在明显差异, 焊核区形成了细小的等轴晶组织; 热机影响区组织发生了弯曲变形, 远离焊核区部分组织发生了回复再结晶; 热影响区组织发生明显粗化. 接头析出相受到焊接热循环和搅拌作用的影响, 在接头各区域的分布形态存在明显差异.

(2) 2219铝合金搅拌摩擦焊接头强度系数可达 70%, 明显优于熔焊接头的力学性能.

(3) 对 2219铝合金 FSW焊缝的显微硬度进行了分析, 结果显示母材硬度最高, 热机影响区和热影响区硬度降低, 到焊核处硬度又升高, 但低于母材的硬度, 最低点位于后退侧热影响区.

(4) 试件多数在后退边热影响区断裂, 成为焊接接头的最薄弱环节, 接头的断裂形式为韧性断裂.

参考文献:

[1] Narayana G V, Sharma V M J, Diwakar V, et al. Fracture behavior of aluminum alloy 2219-T87 welded plates[J]. Science and Technology of Welding and Joining, 2004, 9(2): 121—130.

[2] 陈迎春, 刘会杰, 冯吉才. 2219-O铝合金的搅拌摩擦焊接[J]. 焊接学报, 2006, 27(1): 65—68.
Chen Yingchun, Liu Huijie, Feng Jicai. Friction stir welding of 2219-O aluminum alloy[J]. Transactions of the China Welding Institution, 2006, 27(1): 65—68.

[3] Thomas W M, Nicholas E D. Friction stir welding for the transportation industries[J]. Materials and Design, 1997, 18(4/6): 269—273.

[4] Colegrove P A, Shercliff H R. Experimental and numerical analysis of aluminum alloy 7075-T7351 friction stir welds[J]. Science and Technology of Welding and Joining, 2003, 8(5): 360—368.

[5] Joelj D. The friction stir welding advantage[J]. Welding Journal, 2001, 80(5): 30—34.

[6] Ericsson M, Sandstrom R. Influence of welding speed on the fatigue of friction stir welds, and comparison with MIG and TIG[J]. International Journal of Fatigue, 2003, 25(12): 1379—1387.

[7] 邢 丽, 柯黎明, 刘鸽平, 等. 铝合金 LD10的搅拌摩擦焊组织及性能分析[J]. 焊接学报, 2002, 23(6): 55—58.
Xing Li, Ke Liming, Liu Geping. Microstructure and mechanical properties of a friction stir welded LD10 aluminum[J]. Transactions of the China Welding Institution, 2002, 23(6): 55—58

[8] 傅志红, 贺地求, 周鹏展, 等. 7A52铝合金搅拌摩擦焊焊缝的组织分析[J]. 焊接学报, 2006, 27(5): 65—68.

[下转第 84页]

为全面改善焊条工艺性能提供了方向.

参考文献:

[1] 孙 咸. 焊接有害物质及其对健康的影响[J]. 机械工人(热加工), 2006(8): 17—22.
Sun Xian. Welding hazardous substances and their effects on health[J]. MachinistMetalForming, 2006(8): 17—22.

[2] 张承恩. 均匀设计与参数优化[EB/OL]. [2009—09—13]. http://xyzok.232.lgj.cn/2sjyy.htm.

[3] 孟工戈, 杨拓宇, 刘晓晶, 等. 新渣系碱性焊条脱渣性分析[J]. 焊接学报, 2008, 29(3): 33—36.
Meng Gongge, Yang Tuoyu, Liu Xiaojing, et al. Slag detachability of new slag system basic electrode[J]. Transactions of the China Welding Institution, 2008, 29(3): 33—36.

[4] 上月映野, 成瀬省三. ステンレス鋼被履アーク溶接棒: 日本, 特開 2002—205191[P]. 2002—07—23.

[5] 梅木正夫, 高橋将, 岩立健太郎. 低水素系被履アーク溶接棒: 日本特開 2004—1048[P]. 2004—01—08.

[6] 蒋建敏, 李现兵, 王智慧, 等. 焊接烟尘发尘机理及其影响因素[J]. 焊接, 2006(1): 7—11.
Jiang Jianmin, Li Xianbing, Wang Zhihui, et al. The mechanism and influencing factor of welding fume formation[J]. Welding & Joining, 2006(1): 7—11.

[7] 沈晓勤, 蒙继龙, 宋永伦. 焊接过程中有害物质问题的研究及其进展[J]. 焊接, 2005(7): 5—8.
Shen Xiaoqin, Meng Jilong, Song Yonglun. Research and progress on the problem of welding hazardous subtances[J]. Welding & Joining, 2005(7): 5—8.

[8] 孟工戈, 金龙浩, 赵国华, 等. 新渣系碱性焊条发尘量及发尘速率[J]. 焊接学报, 2007, 28(6): 77—80.
Meng Gongge, Jin Longhao, Zhao Guohua, et al. Weld fume quantity and emission rate of new slag system basic electrode[J]. Transactions of the China Welding Institution, 2007, 28(6): 77—80.

作者简介: 孟工戈, 男, 1956年出生, 硕士, 教授. 主要研究方向为焊接材料及工艺、电子封装无铅钎料等. 发表论文 30余篇.
Email: menggongge@126.com

[上接第 80页]

Fu Zhihong, He Diqiu, Zhou Pengzhan. Structure investigation of friction stir welding of 7A52 aluminum alloy[J]. Transactions of the China Welding Institution, 2006, 27(5): 65—68.

[9] 季亚娟, 蒋成禹, 严 铿. LF5铝合金搅拌摩擦焊工艺及性能研究[J]. 电焊机, 2001, 34(1): 31—33.
Ji Yajuan, Jiang Chengyu, Yan Keng. Process and property in friction stir welding of LF5 aluminum alloy[J]. Electric Welding Machine, 2001, 34(1): 31—33.

[10] 贺地求, 邓 航, 周鹏展. 2219厚板搅拌摩擦焊组织及性能分析[J]. 焊接学报, 2007, 28(9): 13—16.
He Diqiu, Deng Hang, Zhou Pengzhan. Analysis of microstructure and properties in friction-stir welding of 2219 thick plate[J]. Transactions of the China Welding Institution, 2007, 28(9): 13—16.

作者简介: 王春炎, 女, 1985年出生, 硕士. 主要研究方向为 2219铝合金焊接新技术及焊缝性能. 发表论文 5篇.
Email: xiaomin010327@163.com

shows the best mechanical property of the brazed joint, when the Ag content exceeds 3.3%, the mechanical property of the brazed joint remains stable. The addition of Ag can refine the $CuAl_2$ brittle phase in the brazed seam, which decreases the stress concentration and enhances the brazed joints. In general, the brazing filler metal with 3.3% Ag has the best comprehensive properties.

Key words: brazing; Cu-Al; Zn-Al fill metal; spreadability; mechanical property; microstructure

Microstructures and mechanical properties of friction stir welded 2219-T87 aluminum alloy joints WANG Chunyan[1], QU Wenqing[1], YAO Junshan[2], ZHAO Haiyun[1] (1. School of Mechanical Engineering & Automation, Beihang University, Beijing 100191, China; 2. Shanghai Aerospace Equipments Manufacturer, Shanghai 200245, China). p 77—80, 84

Abstract: The joint of 2219-T87 aluminum alloy plate in 8 mm thickness was obtained by friction stir welding (FSW), and the microstructures and mechanical properties of the joint were investigated. The results show that the microstructure in the nugget zone (NZ) consists of refined and equiaxed grains, that in the thermal-mechanically affected zone (TMAZ) consists of deformed grains, and that in the heat affected zone (HAZ) consists of coarse lath grains. There is an obvious interface between NZ and TMAZ at the advancing side, but there is illegibility comparatively at the retreating side. The precipitation phenomena in different zone are affected by friction stir welding. The results of tensile properties show that the transverse tensile strength of FSW joint can reach about 70% of that of the base metal. Hardness measurements show that the FSW joint is soften during welding, heat affect zone has serious softening, and tensile specimens fracture at the HAZ of retreating side. Fractographs confirm that the fracture of the joint is the mode of ductile fracture.

Key words: aluminum alloy 2219; friction stir welding; mechanical properties; microstructures

Comprehensively optimizing usability of new slag system basic electrode MENG Gongge[1], CHU Jijun[2], LUAN Jingyue[3], GU Feng[1], LI Dan[1], ZHANG Zhuanlian[2] (1. School of Material Science & Engineering, Harbin University of Science and Technology, Harbin 150040, China; 2. Harbin Welding Institute, China Academy of Machinery Science and Technology, Harbin 150080, China; 3. Dalian Boiler and Pressure Vessel Inspection Institute, Dalian 116013, China). p 81—84

Abstract: A new slag system was designed after analyzing several domestic and abroad basic slag system electrode coatings. The experiments were arranged by the uniform design method and computer software. Nine coating constituents were taken as independent variables and were divided into 6 levels in all 24 experiments. The 7 usability target data were put into computer to analyze statistically. The results give the mathematic model multinomial between independent variables and functions, which indicate the influence laws of many coating constituents on many targets. With computers and these mathematic models, many usability targets are optimized and the searching data are got, which give directions for improving usability of electrode. This search/calculating method is also a new attempt for improving electrode properties in an all-round way.

Key words: basic electrode; usability; uniform design; optimization

Influences of LaF_3 on microstructure and performance of laser cladding layer in-situ fabricated CHENG Yiyuan[1], WANG Yong[1], HE Qingkun[1], WANG Zhengfang[2] (1. College of Electromechanical Engineering, China University of Petroleum, Dongying 257061, China; 2. Technical Department, Shandong Qilu Petrochemical Machinery Manufacturing Company Limited, Zibo 255400, China). p 85—88, 92

Abstract: In-situ Ni-based TiC composite coatings with LaF_3 were made by laser cladding, and the microstructure, composition profiles, microhardness, wear and corrosion properties of the coatings were analyzed by using electron probe micro-analyzer (EPMA), transmission electron microscope (TEM), scanning electron microscope (SEM), microhardness instrument, M-2000 Friction and Wear Tester and M398 Electrochemical corrosion systems. The results show that after adding moderate rare earth LaF_3, the microstructure presents more homogeneous, the fineness of grain becomes finer, TiC distributes better and heterogeneous phase decreases. When the content of LaF_3 is 1%, the highest microhardness is got; when it is 2%, the optimal wear and corrosion resistance properties are obtained; but when adding excessive rare earth LaF_3, both the microstructure and properties will get worse.

Key words: laser cladding; in-situ fabricated; rare earth LaF_3; TiC pellet

Effect of magnetic field style on microstructure and properties of overlay deposit LIU Zhengjun, LIU Duo, CI Honggang, SONG Xingkui (School of Material Science and Engineering, Shenyang University of Technology, Shenyang 110870, China). p 89—92

Abstract: The Fe5 alloy was overlaid on low carbon steel by plasma arc surfacing with longitudinal magnetic field. The style of magnetic field was changed during surfacing, which was direct magnetic field or alternating magnetic field. After plasma arc surfacing with magnetic field, the scanning electron microscopes, wear loss test, micro-hardness test were used to analyze the effect of magnetic field style on the properties of overlay deposit. The acting mechanism of magnetic field style and parameters on the properties and microstructure of the deposit was researched. The results indicate that the introduced DC/AC magnetic field can give an effective intervention to the properties of the deposit. The active effect of AC magnetic field is better than that of DC magnetic field because the magnetic field can be controlled during AC magnetic field by alternation of magnetic field frequency. The optimal result is acquired when magnetic current is 3 A and magnetic frequency is 10 Hz, and the hardness of the properties is 68 HRC and wear loss is 0.031 8 g.

Key words: plasma arc surfacing; magnetic field style; electromagnetic stirring; microstructure and properties

Influence of processing parameters on performance of friction stir spot welding with re-filling probe hole YAN Keng, FANG Yuan (Provincial Key Laboratory of Advanced